database and to 1.47 for the characters database. However, it must be noted that in our case only two parameters are used to characterise each BP.

Some examples of retrieval results are shown in Figs. 2 – 4. It can be appreciated that recognition is successful even when additional BPs appear, like in the square and elliptic shapes.

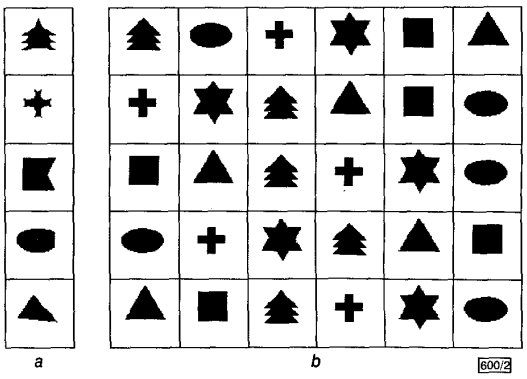

Fig. 2 *Example of HMM recognition*

a Proposed shapes
b Recognition results in order of decreasing similarity

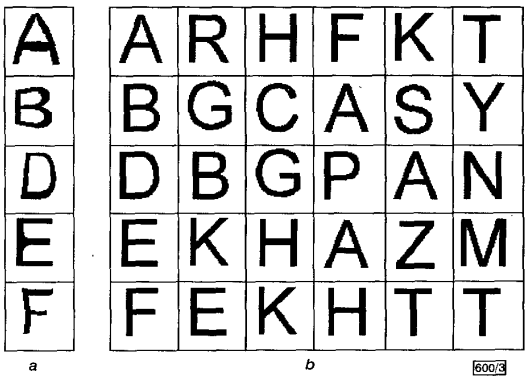

Fig. 3 *Example of HMM recognition*

a Proposed shapes
b Recognition results in order of decreasing similarity

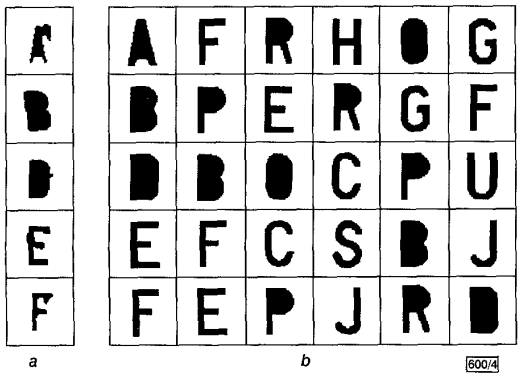

Fig. 4 *Example of HMM recognition*

a Proposed shapes
b Recognition results in order of decreasing similarity

Finally, the main advantage of our method when compared to [1] is that our results are not sensitive to centroid shiftings. Characters in Fig. 4 were extracted from real license plates. In deteriorated and dirty plates, resulting shapes might be seriously deformed and suffer centroid shiftings. Fig. 4 shows how recognition is usually successful even for damaged plates. This property is specially valuable when the objects to be recognised are overlapped.

Conclusions: A new deformed retrieval method based on hidden Markov models has been presented in this Letter. The proposed method is resistant against shape transformations including translation, rotation and scale. Since HMMs are resistant against noise, the algorithm is also flexible to severe non-rigid distortions. Our method requires only two features to characterise each hidden state. Hence, it is computationally less expensive than similar approaches [1]. The efficiency of the method has been proven for several different databases.

Acknowledgments: This work has been partially funded by the Spanish Comisión Interministerial de Ciencia y Tecnología (CICYT), under Project No. T1C098-0562. We would also like to thank F.S. Chang and S.Y. Chen, from Yuan-Ze University (Republic of China), for their help and for providing the databases used in this work.

4 September 2001
Electronics Letters Online No: 20010980
DOI: 10.1049/el:20010980

C. de Trazegnies, F.J. Miguel, C. Urdiales, A. Bandera and F. Sandoval (*Dpto. Tecnología Electrónica, E.T.S.I. Telecomunicación, Universidad de Málaga, Campus de Teatinos, 29071, Málaga, Spain*)

E-mail: carmina@dte.uma.es

References

1 CHANG, F.S., and CHEN, S.Y.: 'Deformed shape retrieval based on Markov model', *Electron. Lett.*, 2000, **36**, (2), pp. 126–127
2 BANDERA, A., URDIALES, C., ARREBOLA, F., and SANDOVAL, F.: 'Corner detection by means of adaptively estimated curvature function', *Electron. Lett.*, 2000, **36**, (2), pp. 124–126
3 RABINER, L.R.: 'A tutorial on hidden Markov models and selected applications in speech recognition', *Proc. IEEE*, 1989, **77**, (2), pp. 257–286
4 HARTIGAN, J.A.: 'A k-means clustering algorithm', *Appl. Stat.*, 1979, **28**, pp. 100–108

Compact atomic clock based on coherent population trapping

J. Kitching, L. Hollberg, S. Knappe and R. Wynands

A simple, compact, low-power physics package for a vapour-cell atomic clock is described. The device measures 6.6 × 1.6 × 1.3 cm and dissipates less than 30 mW of electrical power without thermal control. The instability is $1.3 \times 10^{-10}/\sqrt{[\tau/(s)]}$ for integration times τ below 100 s. Applications for this device include distributed telecommunications systems, advanced global positioning system (GPS) receivers and laboratory instrumentation.

Frequency references based on atomic transitions generally provide far better accuracy and reproducibility than quartz-crystal oscillators. The atomic frequency reference described in this Letter is designed to achieve this goal while simultaneously being simple, compact, and consuming low power. The reference is based on the phenomenon of coherent population trapping (CPT) [1, 2]. Light from a laser is modulated with an external microwave oscillator to produce optical sidebands separated by the atomic ground-state hyperfine frequency. The light is sent through a glass cell containing a thermal vapour of Cs atoms along with a Ne/Ar mixture buffer gas of several kPa. A weak, longitudinal magnetic field is applied to the cell using a small current passed through some coils, to separate the $m_F = 0 \rightarrow m_{F'} = 0$ transition from those involving other ground-state Zeeman levels (see Fig. 1*a*). When the modulation frequency exactly equals a subharmonic of the atomic hyperfine transition frequency (~9.2 GHz for Cs), the absorption of the light through the cell changes. In the system described here, the modulation frequency was 4.6 GHz and the two first-order sidebands form the optical configuration in Fig. 1*a*. The output from a photodetector measuring the change in transmission is used to correct the modulation frequency and lock the external oscillator to the atomic resonance. The long-term stability of the clock is

derived from the insensitivity of the atoms to external perturbations such as temperature and magnetic fields. Clocks based on this all-optical CPT excitation method have been developed previously as large-scale experiments [3 – 5].

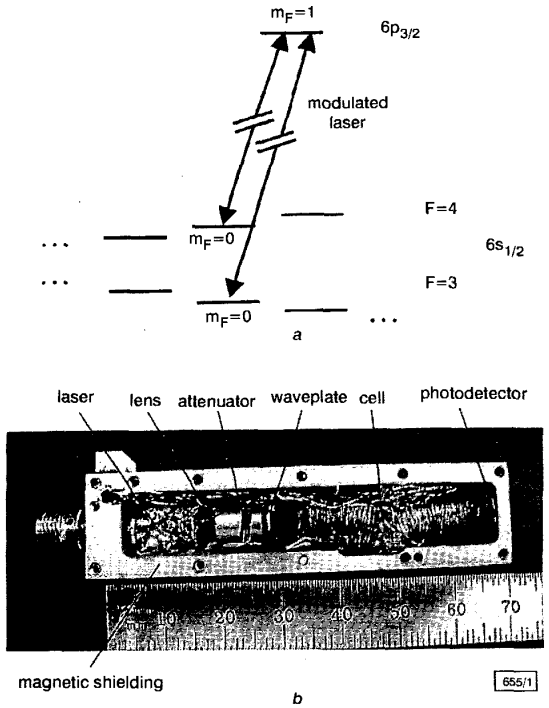

Fig. 1 *Atomic level diagram of Cs^{133} with laser tunings required for all-optical excitation of atoms and photograph of compact physics package with volume < 15 cm^3*

a Atomic level diagram
b Photograph of compact package

Fig. 1*b* shows a photograph of the compact system. A vertical-cavity surface-emitting laser (VCSEL) emits light near the 852 nm optical transition in Cs. The laser is temperature-stabilised and its wavelength locked to the atomic transition with feedback to the injection current. A small lens collimates the light, its power is attenuated, and a quarter-wave plate changes the polarisation from linear to circular. The light then passes through the Cs cell, which has an inner diameter of 4 mm and a length of 25 mm. Finally a slow Si *PIN* photodiode placed behind the cell measures the transmitted optical power. All components are contained in a structure machined out of a metal of high magnetic permeability to shield the cell from external magnetic fields. In addition, the laser package was found to be magnetic at a level sufficient to affect the atoms. It is therefore placed inside a magnetic shield of its own, with a 1 mm hole through which the light exits. The microwave modulation signal is brought to the laser through an SMA connector and non-magnetic semi-rigid coaxial cable.

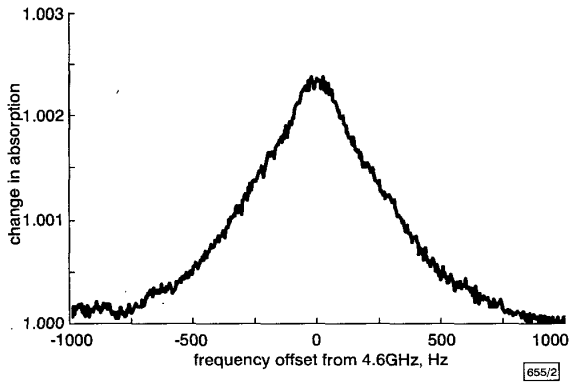

Fig. 2 *Dark-line CPT resonance at 4.6 GHz*

As the microwave frequency is swept near the atomic transition, the DC power is measured at the photodetector, as shown in Fig. 2. The resonance width is roughly 600 Hz at 4.6 GHz, somewhat larger than that reported previously [5]. This is due in part to the smaller cell size: the atomic coherence lifetime is reduced, and the microwave transition broadened, because of collisions of the atoms with the cell walls. The microwave oscillator (crystal oscillator and frequency synthesiser) is then locked to the atomic resonance using lock-in detection. With the system locked, the output frequency at 4.6 GHz is measured relative to a hydrogen maser as a function of time, and the Allan deviation, shown in Fig. 3, is calculated. The Allan deviation shows a short-term fractional frequency instability of $1.3 \times 10^{-10}/\sqrt{[\tau/(s)]}$. This is about an order of magnitude larger than that measured with a large-scale system but is quite good for a small system that has not yet been optimised. This increased instability is predominantly a result of the broader resonance line. At longer integration times, we believe that the variations of the atomic-transition frequency could be caused by uncontrolled temperature changes of the cell.

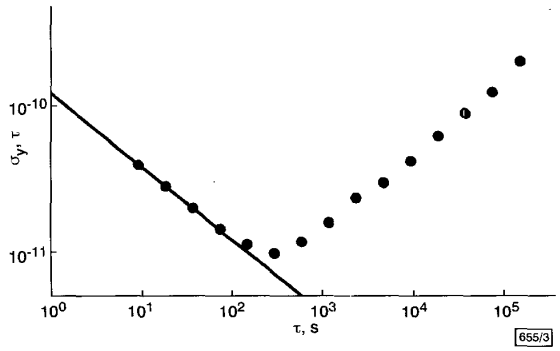

Fig. 3 *Allan deviation of locked frequency reference*

● experimental data
——— $1.3 \times 10^{-10}/\sqrt{(\tau/s)}$

For atomic clock applications, VCSELs offer several advantages over conventional edge-emitting lasers. The first is low-power operation: singlemode VCSELs have a threshold current of less than 1 mA and require only a few milliwatts of DC power to operate. In addition, because of their large modulation bandwidth, the PF power required to produce large optical sidebands is small (~20 mW). Aside from thermal control of the laser and cell, no other significant power is required to operate the physics package. Another advantage is reliability and operation free from mode-hops. We have been able to keep the system running for many days without servos unlocking as a result of laser mode-hops. Improvements in both the size and stability of the device also appear possible. The use of a shorter cell at a higher temperature, an unpackaged laser that does not require magnetic shielding, and the reduction of excess space between the components would reduce the overall length to roughly one-third of its current value. An increase in the buffer-gas pressure would reduce the diffusion constant of the Cs in the cell and isolate the atoms more from the cell walls, although some accompanying reduction in signal size would be expected. We anticipate a reduction in the instability by a factor of ~3. Finally, active temperature stabilisation of the cell would be likely to improve the long-term frequency stability.

Compact atomic clocks have been previously developed using conventional optical-microwave double-resonance methods [6, 7], in which the cell is placed inside a microwave cavity. These clocks have short- and long-term instabilities comparable to those measured here and physics package volumes of the order of 1 cm^3. However, the prospects for further miniaturisation of these conventional designs appear limited because the microwave cavity must be roughly the size of the microwave wavelength (~3 cm for Cs) in order to be resonant. Miniaturisation of the all-optical excitation design presented here appears straightforward, and is limited fundamentally only by the size of the optical wavelength (~1 μm). Smaller volumes lead to operation at lower power (due to reduced heat required for temperature control) and often lower production cost. Such clocks may be useful in a variety of military [8] and civilian [9] applications.

7 September 2001
Electronics Letters Online No: 20010959
DOI: 10.1049/el:20010959

J. Kitching and L. Hollberg (*The Time and Frequency Division, NIST, 325 Broadway, Boulder, CO 80305, USA*)

S. Knappe and R. Wynands (*Institut für Angewandte Physik, Universität Bonn, D-53115, Bonn, Germany*)

References

1 ALZETTA, G., GOZZINI, A., MOI, L., and ORRIOLS, G.: 'An experimental method for the observation of RF transitions and laser beat resonances in oriented Na vapor', *Nuovo Cim.*, 1976, **B 36**, pp. 5–20
2 ARIMONDO, E., and ORRIOLS, G.: 'Nonabsorbing atomic coherences by coherent two-photon transitions in a three-level optical pumping', *Lett. Nuovo Cim.*, 1976, **17**, pp. 333–338
3 THOMAS, J.E., EZEKIEL, S., LEIBY, C.C., Jr., PICARD, R.H., and WILLIS, C.R.: 'Ultrahigh-resolution spectroscopy and frequency standards in the microwave and far-infrared regions using optical lasers', *Opt. Lett.*, 1981, **6**, pp. 298–300
4 CYR, N., TETU, M., and BRETON, M.: 'All-optical microwave frequency standard: a proposal', *IEEE Trans. Instrum. Meas.*, 1993, **42**, pp. 640–649
5 KITCHING, J., KNAPPE, S., VUKICEVIC, N., HOLLBERG, L., WYNANDS, R., and WEIDEMANN, W.: 'A microwave frequency reference based on VCSEL-drive dark line resonances in Cs vapor', *IEEE Trans. Instrum. Meas.*, 2000, **49**, pp. 1313–1317
6 CHANTRY, P.J., LIBERMAN, I., VERBANETS, W.R., PETRONIO, C.F., CATHER, R.L., and PARTLOW, W.D.: 'Miniature laser-pumped cesium cell atomic clock oscillator'. Proc. 1996 IEEE Int. Frequency Control Symp., 1996, pp. 1002–1010
7 BLOCH, M., PASCARU, I., STONE, C., and McCLELLAND, T.: 'Subminiature rubidium frequency standard for commercial applications'. Proc. 1993 IEEE Int. Frequency Control Symp., 1993, pp. 164–177
8 VIG, J.R.: 'Military application of high accuracy frequency standards and clocks', *IEEE. Trans. Ultrason. Ferr. Freq. Control*, 1993, **40**, (5), pp. 522–527
9 KUSTERS, J.A., and ADAMS, C.A.: 'Performance requirements of communication base station time standards', *RF Oscillators*, May 1999, pp. 28–38

Microelectromechanical capacitor with wide tuning range

H. Nieminen, V. Ermolov and T. Ryhänen

A new anchoring design is proposed for a microelectromechanical (MEM) capacitor that allows realisation of wide tuning range devices. The MEM capacitor is made of gold using surface micromachining. The capacitor has a capacitance of 1.58 pF and achieves a tuning range of 2.25:1 with parasitics.

Introduction: Voltage controlled capacitors are key elements in many microwave and millimetre wave applications, for example tunable matching networks, voltage controlled filters, and voltage controlled oscillators (VCOs) [1, 2]. The variable capacitors that are required in these applications can be implemented with *pn*-junctions [3]. However, since these applications require a high quality factor (Q) and a wide tuning range [2], it has been proposed that metallic surface micromachined microelectromechanical (MEM) capacitors could be used [4, 5]. The main advantages of the MEM capacitor are the low series resistance when metal is used as a structural material, the ability to keep the signal circuit apart from the control circuit, and mechanical inertia that isolates the mechanical dynamics from the radio frequency electrical signals.

MEM capacitor: A voltage controlled MEM capacitor usually consists of two electrodes. One is fixed to the substrate and the other suspended over the fixed electrode using mechanical springs. When the bias voltage is applied between the electrodes, electrostatic force attracts the suspended electrode towards the fixed electrode. The bias voltage attracts the suspended electrode towards the bottom electrode until equilibrium between the mechanical spring force and the electrical force is reached. Since the spring force is a linear function of the gap and the electric force is inversely proportional to the second power of the gap, there is a stable equilibrium point only when the air-gap is more than 2/3 of the original air-gap. Therefore, the theoretical maximum capacitance tuning range of the one-gap structure is limited to 50%. However, the tuning range can be increased using a two-gap structure with separate control and signal electrodes [5]. Fig. 1 shows the operational principle of a one-gap and a two-gap MEM capacitor. If, in the two-gap structure, the gap between the control electrode and the suspended electrode is three times larger than the gap between signal electrode and the suspended electrode, the control voltage pull-in does not limit the maximum tuning range.

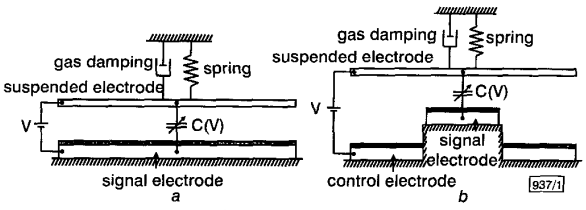

Fig. 1 *Functional models of one-gap and two-gap MEM capacitors*

a One-gap MEM capacitor
b Two-gap MEM capacitor

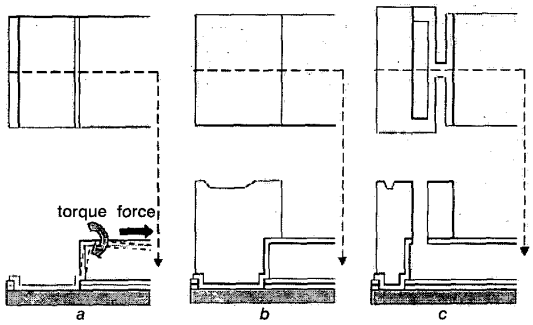

Fig. 2 *Torque on suspended membrane owing to stress induced force, proposed firm anchoring structure using thick electroplating and advanced anchoring structure using thick electroplating to form springs having low series resistance*

a Torque on membrane
b Proposed anchoring structure
c Advanced anchoring structure

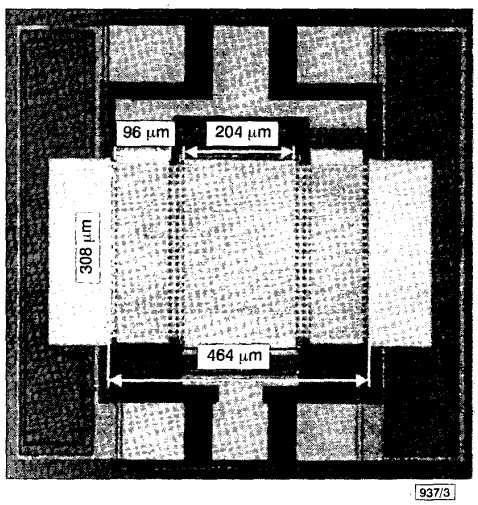

Fig. 3 *Photograph of two-gap tunable MEM capacitor with firm anchoring*

Nominal air-gaps of signal and control electrodes are 0.5 and 1.5 μm, respectively

The problem with the MEM capacitor is that to achieve capacitance values suitable for the above-mentioned applications [1, 2] within reasonable device area, the air gap has to be controlled